

## Gamma-ray energies from the reaction $^{35}\text{Cl}(n,\gamma)$

E. G. Kessler, Jr., G. L. Greene, and R. D. Deslattes

*Center for Basic Standards, National Bureau of Standards, Gaithersburg, Maryland 20899*

H. G. Börner

*Institut Laue-Langevin, F-38042 Grenoble Cedex, France*

(Received 17 December 1984)

A two-axis flat-crystal spectrometer has been used to measure accurately gamma-ray energies up to 2 MeV from the reaction  $^{35}\text{Cl}(n,\gamma)$ . This represents a fourfold extension of the range of direct optically based gamma-ray energies. The crystals and spectrometer have performed in a manner which demonstrates that sub-ppm measurements are possible at energies  $\geq 2$  MeV. The reported transition energies (in eV) are  $517\,077.41 \pm 0.23$ ,  $786\,311.32 \pm 0.38$ ,  $788\,437.43 \pm 0.44$ ,  $1\,164\,885.74 \pm 0.48$ ,  $1\,951\,197.06 \pm 0.58$ , and  $1\,959\,413.45 \pm 8.45$ . The sum rule is satisfied by three of the lines ( $786\text{ keV} + 1165\text{ keV} = 1951\text{ keV}$ ) within an uncertainty of  $\sim 1$  ppm.

### I. INTRODUCTION

Gamma-ray secondary standards for  $E < 1.0$  MeV have been most accurately measured using intense radioactive sources and flat crystal spectrometers whose energy (wavelength) scale was directly related to optical wavelengths. Previously published results include lines resulting from the decay of  $^{198}\text{Au}$ ,  $^{192}\text{Ir}$ ,  $^{169}\text{Yb}$ , and  $^{170}\text{Tm}$ .<sup>1,2</sup> The highest energy which was directly measured in any of these studies was the  $^{198}\text{Au}$  675 keV line and the uncertainties were  $\sim 0.5$  to 1.0 ppm.

These lines have been used together with precision curved crystal spectrometer (ratio) measurements to establish consistent gamma-ray markers for the energy regions 0–1.3 MeV and 1.3–3.5 MeV.<sup>3,4</sup> The energy scale of the standards in both regions is thus based on the flat crystal measurements. Standards in the lower region generally involve one relative measurement while standards in the higher region generally involve two or three relative measurements.

All of the above-mentioned flat crystal sources were sufficiently long lived ( $T_{1/2} > \text{a few days}$ ), so that samples could be activated in a reactor and transported to a laboratory area specifically equipped for precision measurements. Because the spectrometer's high resolution is necessarily associated with low efficiency (a few  $\times 10^{-11}$ ), only the most intense gamma-ray lines can be conveniently measured. For  $E > 1$  MeV intense gamma-ray lines are only available from the prompt decay of a nucleus following thermal neutron capture. The sample must reside in the reactor during measurement, and the spectrometer must be in close proximity to the reactor. The high flux reactor at the Institut Laue-Langevin (ILL) provides a unique facility for such  $(n,\gamma)$  measurements because (1) it has a high neutron flux ( $5 \times 10^{14}$  n cm<sup>-2</sup> s<sup>-1</sup>); (2) access is available to a tangential reactor port; and (3) facilities to change sources while the reactor is in operation exist.

Our purpose in extending flat crystal measurements to these higher energies is the general improvement of secondary standards in the 2–3 MeV region. In addition, we

hope to obtain an improved value for the neutron mass by measuring the 2.2 MeV gamma ray emitted from the reaction  $^1\text{H}(n,\gamma)^2\text{H}$ , and to determine the combination of fundamental constants  $N_A h/c$  (Ref. 5). It is possible in this way to obtain a relatively model-independent value for the fine structure constant  $\alpha$ .

The precision spectrometer was constructed and extensively tested at the NBS before being moved to the ILL. Measurements reported here on  $^{35}\text{Cl}$  were recorded during the first runs dedicated to the flat crystal spectrometer. They provide accurate energy standards up to  $\sim 2$  MeV, establish limits on perfection of the crystals used for diffraction, and demonstrate the capability of the entire spectrometer to make precision measurements in the 2 MeV energy range and above.

### II. EXPERIMENTAL PROCEDURES

#### A. Source

Granulated high purity NaCl of natural composition ( $^{35}\text{Cl}$ —75.5%,  $^{37}\text{Cl}$ —24.5%) was placed in a graphite target holder. The NaCl volume was  $0.25 \times 1.3 \times 2.5$  cm<sup>3</sup> and the mass was 1.8 g. The capture cross section for  $^{35}\text{Cl}$  is  $\sigma = 44$  b. The reader is referred to Ref. 6 for details of the ILL in-pile source assembly.

#### B. Measurement chain

Three steps are involved in the measurement chain which links the gamma-ray wavelengths to visible wavelengths. These steps have been discussed in full detail in Ref. 7. In the first step, the lattice spacing of a Si crystal is measured in terms of the wavelength of an iodine stabilized HeNe laser operating in the visible near 633 nm. This step employs simultaneous x-ray and optical interferometry and yields a calibrated Si crystal sample.

In the second step, the lattice spacings of various other crystals are compared to the calibrated Si crystal to yield a family of crystals whose lattice spacings are known rela-

tive to the optical wavelength. This method employs an x-ray crystal comparator. Diffraction geometries which are nearly nondispersive are used so that there is negligible dependence on the x-ray wavelengths used.

In the final-step, gamma rays are diffracted by the crystals calibrated in step two and the diffraction angles are accurately measured. By combining the measured lattice spacing and diffraction angles, gamma-ray wavelengths are determined. The measurements of the Cl  $\gamma$  rays reported here are the combination of new diffraction angle measurements and previous lattice spacing measurements.<sup>7</sup>

### C. Gamma-ray spectrometer

The spectrometer used to measure the diffraction angles is a two-axis flat-crystal instrument with crystals in transmission geometry. Gamma rays from the source pass through a slit collimator, are diffracted by the first crystal, pass through an intercrystal collimator, are diffracted by the second crystal, pass through a third collimator, and are then detected. The diffraction angles are quite small at these energies ( $0.13^\circ$  at 1.95 MeV in first order) so the slit collimators need to have a restricted angular acceptance in order to prevent the direct beam from entering the detector. The openings of the slit collimators are such that only the central 1 mm wide crystal region is used for diffraction.

The first crystal is approximately 15 m from the source and the two crystals are separated by 53 cm. Because the source is stationary, the entire spectrometer rotates about the first crystal axis, and the detector rotates about the second crystal axis.

The diffraction angles are measured by polarization-sensitive Michelson interferometers having a sensitivity and accuracy of a few  $\times 10^{-4}$  arcsec ( $\sim 10^{-9}$  rad). The angle interferometers were calibrated by summing to closure the external angles of an optical polygon. Complete details of a similar spectrometer, its angle interferometers, and the calibration procedure are available in Ref. 7

### D. Crystals

The crystals used were 5 cm wide  $\times$  2.5 cm high  $\times$   $\sim$  5 mm thick slabs of Ge oriented with the (400) planes available for diffraction. They were mounted on posts of Ge in a manner which minimizes strains. Optical references provide alignment of the crystal planes with respect to the axis of rotation to  $< 2$  arcsec.

The diffraction of high energy (short wavelength) gamma rays puts very stringent requirements on crystal perfection. Using dynamical theory of diffraction for perfect crystals,<sup>8</sup> the product of the energy and the width ( $Ew$ ) can be shown to equal  $2d(F/V)$  (45.87) keV arcsec, where  $E$  is the gamma-ray energy in keV,  $w$  is the FWHM in arcsec,  $d$  is the lattice spacing in  $\text{\AA}$  and  $F$  is the structure factor for the unit cell of volume  $V$  in  $\text{\AA}^3$ . Our data on diffraction widths and intensities show no detectable deviation from this ideal behavior up to  $\sim 2$  MeV. A more complete discussion of the observed behavior of perfect crystal diffraction up to 2 MeV will be given in a future paper.

The measured lattice spacing of the Ge (400) crystals has previously been reported to be  $0.565\,782\,16\text{ nm} \pm 0.14$  ppm at  $22.5^\circ\text{C}$  (Ref. 7). This value, along with an expansion coefficient  $\alpha_{\text{Ge}} = 5.95 \pm 0.11 \times 10^{-6} \text{K}^{-1}$ , was used in the determination of gamma-ray energies.

### III. DATA ANALYSIS AND RESULTS

For each energy and order number, rocking curves were recorded with the first and second crystals in the parallel and antiparallel positions. The first crystal was held fixed while the second crystal was step scanned in angle. The parallel and antiparallel profiles were fit with a Lorentzian function and a convolution of a Lorentzian with a vertical divergence function, respectively. The correction for vertical divergence is very small ( $< 0.2$  ppm) because the source is  $\sim 2$  cm high and 15 m from the first crystal. A typical scan is displayed in Fig. 1. Each data run consisted of a number of parallel and antiparallel scans. The parallel scans effectively measure the optical fringe positions at which the diffracting planes of first and second crystal lattices are parallel. These were fit to a second order polynomial in time. This provided an estimate of the (slowly) drifting reference position from which the fringe positions of the antiparallel rocking curves were determined. The second column of Table I contains the number of antiparallel rocking curves in each run.

The calibration constant for the interferometer is used to convert interferometer fringes to angles. The interferometer was calibrated eight times since the spectrometer was installed at ILL. The last four calibrations which were completed before and after the recording of the chlorine data show a smooth variation with time and were used to determine daily calibration constant values for converting fringes to angles. The calibration constant exhibits a temporal drift of  $\sim 2$  ppm/yr. In addition, the temperature dependence of the interferometer constant was measured to be  $0.94$  ppm/ $^\circ\text{C}$ .

The interferometer fringe data, the calibration constant, and the measured lattice spacing have been combined to

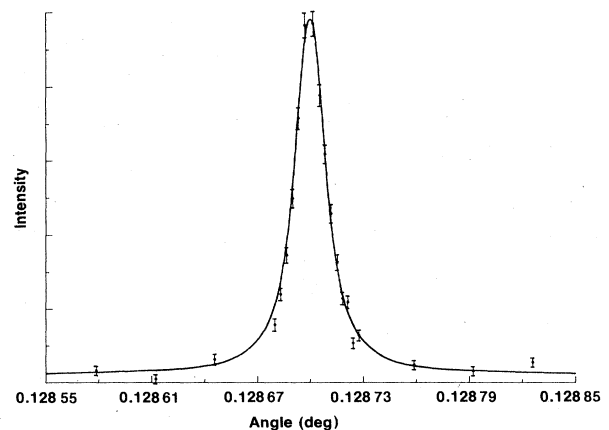


FIG. 1. Double crystal profile of the 1951 keV line using the Ge 400 reflection. The FWHM  $\Delta\theta = 0.065$  arcsec and the resolution  $\theta/\Delta\theta \approx 7000$ .

TABLE I.  $^{36}\text{Cl}$  gamma-ray energies in electron volts. First column: 400—both crystals in first order, 800—both crystals in second order, 400/800—first crystal in first order, second crystal in second order. Second column: number of antiparallel scans. Third column: average energy for run. Fourth, fifth, and sixth columns: average energy, statistical error, and total error for the gamma line.

Order	Scans	Measured energy	Average energy	$\sigma_m$	$\sigma_t^a$
400	7	517073.20±0.23			
400	5	517073.95±0.31			
800	6	517073.66±0.04			
800	4	517073.02±0.07	517073.42	0.10	0.23 (0.44 ppm)
800	15	517073.28±0.02			
800	10	517073.28±0.08			
800	10	517073.36±0.06			
800	4	517073.66±0.14			
800	4	517073.33±0.12			
400	5	786301.94±0.37			
400	4	786302.41±0.44	786302.07	0.23	0.39 (0.50 ppm)
800	7	786301.47±0.30			
800	5	786302.47±0.57			
400	7	788428.38±0.68			
400/800	4	788427.54±0.27	788428.15	0.31	0.44 (0.56 ppm)
800	5	788428.54±0.39			
400	6	1164865.53±0.93			
400	6	1164865.81±0.72	1164865.46	0.21	0.51 (0.44 ppm)
800	4	1164865.66±1.09			
800	4	1164864.86±0.56			
400	6	1951143.32±2.80			
400	6	1951141.17±2.00			
400/800	8	1951136.49±1.20	1951140.46	1.12	1.37 (0.70 ppm)
400/800	4	1951141.23±1.79			
800	4	1951140.12±1.33			
400	8	1959356.16±8.41	1959356.16	8.41	8.45 (4.31 ppm)

<sup>a</sup>The uncertainties do not include any contributions for the voltage-wavelength conversion factor (2.6 ppm) or for the discrepancy (1.8 ppm) between the NBS and PTB measurements of the Si lattice spacing. These values are based on a Si lattice spacing of  $a_0 = 543\,102.997$  fm (22.5°C in vacuum) which also provides the scale for all other  $\gamma$ -ray measurements in this energy range.

determine a gamma-ray wavelength for each run. These wavelengths have been converted to energies using the conversion factor  $V\lambda = 1.239\,852\,0 \times 10^{-6}$  eV m exactly.<sup>9</sup> The third column of Table I contains these energies. If comparisons with energies based on purely electrical standards are needed, it may be necessary to add an additional error of 2.6 ppm in quadrature to our quoted results. The reader is referred to Ref. 7 for a more complete discussion of this question.

For each of the several gamma lines we have obtained a variety of runs in different orders with varying statistical uncertainties (the third column of Table I). The usual procedure to combine independent measurements of fundamental quantities and their uncertainties involves weighting the measurements according to statistical uncertainties (weight =  $1/\sigma^2$ ). Such a procedure gives very different weights to the measurements reported in the third column of Table I. (For example, the ratio of the weights of the fifth and second entries for the 517 keV

line is more than 200, while the ratio of the weights of the fourth and third entries for the 1165 keV line is more than 3.7.) In our opinion, such drastically different weights do not reflect the experimental situation. We have thus chosen to regard the entries in the third column as equal independent measurements and to obtain an uncertainty using the usual root-mean-square procedure. Our best estimate for the energies and statistical uncertainties in the fourth and fifth columns of Table I were obtained using these procedures. The assumption of equal weights as opposed to weighting by statistical uncertainties results in larger uncertainties for all lines except 1165 keV. Since there was only one run for the 1959 keV line, the third column and the fourth and fifth columns are identical.

Total uncertainties (sixth column, Table I),  $\sigma_t$ , are obtained by adding in quadrature the statistical and systematic uncertainties. The estimated systematic uncertainties are calibration—0.2 ppm, temperature—0.3 ppm,

TABLE II.  $^{36}\text{Cl}$  energy comparisons and transition energies.

Laboratory energy (eV)		Recoil energy (eV)	Transition energies	
This work	Krusche <i>et al.</i>		(direct measurement) (eV)	(best estimate) (eV)
517 073.42±0.23	517 077±2	3.99	517 077.41±0.23	517 077.41±0.23
786 302.07±0.39	786 303±3	9.23	786 311.30±0.39	786 311.32±0.38 <sup>a</sup>
788 428.15±0.44	788 433±4	9.28	788 437.43±0.44	788 437.43±0.44 <sup>a</sup>
1 164 865.46±0.51	1 164 870±5	20.25	1 164 885.71±0.51	1 164 885.74±0.48
1 951 140.46±1.37	1 951 146±6	56.81	1 951 197.28±1.37	1 951 197.06±0.58 <sup>a</sup>
1 959 356.16±8.45	1 959 355±6	57.29	1 959 413.45±8.45	1 959 413.45±8.45
Transitions (keV)		Ritz combination energy (eV)		
1951–1165		786 311.56±1.46		
1951–786		1 164 885.98±1.42		
786+1165		1 951 197.01±0.64		

<sup>a</sup>Statistically weighted average of the direct and combination values.

lattice spacing—0.14 ppm, and barometric pressure—0.1 ppm.

The NBS measurement of the lattice spacing of Si differs by 1.8 ppm from a similar measurement at the Physikalisch-Technische Bundesanstalt (PTB) in the Federal Republic of Germany.<sup>10</sup> The NBS result is  $a_0 = 543\,102.997\text{ fm} \pm 0.1\text{ ppm}$  (at 22.5°C, in vacuum) while the PTB result is  $a_0 = 543\,102.018\text{ fm} \pm 0.06\text{ ppm}$  (also at 22.5°C, in vacuum). Intercomparison of crystal samples from NBS and PTB suggests that the lattice spacings are equal to within 0.2 ppm (Ref. 11). However, the intercomparisons to date have involved several steps, intermediate transfer crystals, and contiguous samples extracted from the same boule as the interferometrically measured crystals. Efforts to understand the origin of this apparent discrepancy are under way and robust lattice spacing measurements accurate to  $\leq 0.1\text{ ppm}$  should be available in the near future. No systematic uncertainty has been included for the NBS-PTB Si lattice spacing difference. We note that the existing gamma-ray wavelength scale based on the Au 411 keV line is related to the NBS lattice spacing measurement.

#### IV. DISCUSSION AND CONCLUSIONS

Table II compares the energies reported in Table I with curved crystal spectrometer results of Krusche *et al.*<sup>12</sup> Krusche *et al.* compared the 517 keV line directly to the  $^{198}\text{Au}$  411 keV line in order to establish the energy scale for the curved crystal spectrometer. The curved and flat crystal measurements show no significant discrepancies, although the uncertainty is quite large for some of the curved crystal measurements. Consistency of the curved

and flat crystal measurements is to be expected since the 411 keV reference line was obtained with the same crystals used here and with a similar spectrometer.

By adding recoil energies to measured energies, transition energies result which can be used to ask whether the measurements satisfy the sum rule. In Table II, recoil energies and transition energies for the flat crystal measurements are listed. Three of the transitions are related by the combination principle: 786 keV + 1165 keV = 1951 keV. Energies obtained by applying the combination principle are included in Table II, and these indirectly determined energies are combined with the directly measured values to obtain “best estimate” transition energies.

In summary, a two axis flat crystal spectrometer has been used to measure gamma-ray energies up to the 2 MeV region. The energies are accurate to  $\leq 1\text{ ppm}$ , are directly related to optical wavelengths, and are consistent as shown by the sum rule. Experimental apparatus and techniques have been demonstrated to be adequate for sub-ppm energy measurements in the 2–3 MeV region.

#### ACKNOWLEDGMENTS

We wish to express our appreciation to the director and staff of the Institut Laue-Langevin for providing extensive and efficient assistance in this cooperative effort. In particular we wish to acknowledge the help we received from F. Hoyler and P. Geltenbort for assistance in source preparation and setup. We also wish to thank E. Bauer for his guidance in source design, J. Coquin for his engineering design work, and D. Wheeler and the EDEX Division for continued support throughout the measurement.

<sup>1</sup>E. G. Kessler, Jr., R. D. Deslattes, A. Henins, and W. C. Sauder, *Phys. Rev. Lett.* **40**, 171 (1978).

<sup>2</sup>E. G. Kessler, Jr., L. Jacobs, W. Schwitz, and R. D. Deslattes, *Nucl. Instrum. Methods* **160**, 435 (1979).

<sup>3</sup>R. G. Helmer, R. C. Greenwood, and R. J. Gehrke, *Nucl. Instrum. Methods* **155**, 189 (1978).

<sup>4</sup>R. C. Greenwood, R. G. Helmer, and R. J. Gehrke, *Nucl. Instrum. Methods* **159**, 465 (1979).

<sup>5</sup>R. D. Deslattes, G. L. Greene, and E. G. Kessler, Jr., *J. Phys. (Paris)* **45**, C3-41 (1984).

<sup>6</sup>H. R. Koch, H. G. Börner, J. A. Pinston, W. F. Davidson, J. Faudou, R. Roussille, and O. W. B. Schult, *Nucl. Instrum.*

- Methods 175, 401 (1980).
- <sup>7</sup>R. D. Deslattes, E. G. Kessler, W. C. Sauder, and A. Henins, *Ann. Phys. (N.Y.)* **129**, 378 (1980).
- <sup>8</sup>B. W. Batterman and H. Cole, *Rev. Mod. Phys.* **36**, 681 (1964).
- <sup>9</sup>E. R. Cohen and B. N. Taylor, *J. Phys. Chem. Ref. Data* **2**, 663 (1973).
- <sup>10</sup>P. Becker, K. Dorenwendt, G. Ebeleng, R. Lauer, W. Lucas, R. Probst, H.-J. Rademacher, G. Reim, P. Seyfried, and H. Siegert, *Phys. Rev. Lett.* **46**, 1540 (1981).
- <sup>11</sup>P. Becker, P. Seyfried, and H. Siegert, *Z. Phys. B* **48**, 17 (1982).
- <sup>12</sup>B. Krusche, K. P. Lieb, H. Daniel, T. Von Egidy, G. Barreau, H. G. Börner, R. Brissot, C. Hofmeyr, and R. Rascher, *Nucl. Phys. A* **386**, 245 (1982). (Please note that the energies given in Table 4 have not been corrected for recoil.)